

Analytical formulas for the velocity field induced by an infinitely thin vortex ring

Sam S. Yoon^{1,*} and Stephen D. Heister^{2,†}

¹*Sandia National Laboratories, Fire Science & Technologies, P.O. Box 5800, Albuquerque,
NM 87185-1135, U.S.A.*

²*School of Aeronautics and Astronautics, Purdue University, West Lafayette,
IN 47906-2023, U.S.A.*

SUMMARY

Three different analytical solutions are presented for a potential vortex ring using three different streamfunctions. Verification studies confirm that all three approaches are valid. It is found that the solution obtained using the Biot–Savart law is the most efficient method due to its simplicity. It is shown that all analytical results are accurate to within machine accuracy and sample calculations are included. Copyright © 2004 John Wiley & Sons, Ltd.

KEY WORDS: vortex ring; streamfunction; Biot–Savart law

1. INTRODUCTION

The ring vortex is one of the classical potential flow solutions and has been used in numerous applications in modelling fluid flows. For example, it is well known that a vortex ring can be generated at an orifice exit when a piston (vortex ring generator) moves through a circular tube. The resulting multiple vortex rings interact dynamically while they are streaming downstream. The effect of such motion (instability) is of great interest to fluid dynamicists. Thus it is, in practical application, generally useful to be able to compute velocities induced by the vortex at arbitrary field points. There are three approaches to obtain the analytical solutions of the vortex ring; applying the Cauchy–Riemann equation to the streamfunctions and direct evaluation of Biot–Savart law. Even though all three approaches have been well known to the fluid mechanics community, their exact solutions for any arbitrary field point are not readily available in any standard fluid mechanics texts. Lamb [1] derives the streamfunction, ψ , of the axisymmetric vortex ring and defines the Cauchy–Riemann condition.

*Correspondence to: S. S. Yoon, Sandia National Laboratories, Fire Science & Technologies, P.O. Box 5800, Albuquerque, NM 87185-1135, U.S.A.

†E-mail: ssyoon@sandia.gov

‡E-mail: heister@ecn.purdue.edu

No further derivation is performed. The analysis by Ramsey [2] is almost identical to Lamb's. Duncan *et al.* [3] provides the induced axial velocity at the centre of the vortex ring using the direct evaluation of the Biot–Savart law. However, the general solution at any arbitrary point is not available. Robertson [4] also gives the analytic expression for $u_z(r=0)$ which is in agreement with that of Duncan *et al.* [3]. Karamcheti [5] derives the integral expression of the Biot–Savart law and provides the analytic solution of the infinitely long line-vortex, not the round axisymmetric vortex ring. The streamfunction analysis by Batchelor [6] and Saffman [7] is similar to that of Lamb [1] and Ramsey [2]. Panton [8] also presents the Biot–Savart law whose solution is exactly the same as that of Karamcheti [5]. More recently, Nitsche and Krasny [9] have utilized the streamfunction approach and provided analytical solutions for induced velocities at any general location. We used a different the streamfunction (from the one Nitsche and Krasny [9] used) under the presumption that we should obtain the same results. In principle, the direct evaluation of the Biot–Savart law should also yield the analytical expressions for the vortex ring-induced velocities because the induced velocities, \mathbf{u} , is a curl of the streamfunction, $\Psi = (\psi/r)\hat{e}_\theta$ (for axisymmetric case) which satisfies the continuity equation for incompressible flows. With these motivations, the analytical solution using Biot–Savart law was also attempted. In this paper, we develop a fully analytic solutions, thereby removing the necessity to perform a numerical quadrature and shows there are various ways to obtain the analytical solutions of a filament potential vortex ring.

2. ANALYTIC SOLUTIONS USING THE STREAMFUNCTION

For incompressible fluid, the continuity equation for axisymmetric case can be written as

$$\nabla \cdot \mathbf{u} = \frac{\partial u_z}{\partial z} + \frac{1}{r} \frac{\partial}{\partial r}(ru_r) = 0 \quad (1)$$

For irrotational flows, we choose to determine the velocity \mathbf{u} in terms of the curl of a vector Ψ

$$\mathbf{u} = \nabla \times \Psi \quad (2)$$

where $\Psi = (\psi/r)\hat{e}_\theta$ and ψ is a scalar streamfunction. The expanded form of Equation (2) is

$$\mathbf{u} = \nabla \times \left(\frac{\psi}{r} \right) \hat{e}_\theta = \frac{1}{r} \frac{\partial \psi}{\partial r} \hat{e}_z - \frac{1}{r} \frac{\partial \psi}{\partial z} \hat{e}_r \quad (3)$$

Thus

$$u_z = \frac{1}{r} \frac{\partial \psi}{\partial r}, \quad u_r = -\frac{1}{r} \frac{\partial \psi}{\partial z} \quad (4)$$

This Cauchy–Riemann condition derived in Equation (4) satisfies the continuity Equation (1) and the corresponding streamfunction, ψ , can be written in various ways.

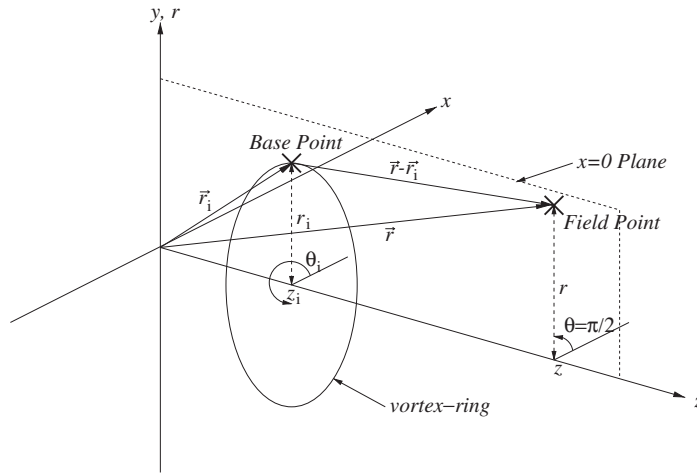


Figure 1. A schematic of vortex-ring geometry for computing induced velocities at arbitrary field points.

Figure 1 highlights the applicable geometry required to compute velocities at a ‘field point’, z, r subject to a ring vortex located at a point z_i, r_i . Nitsche and Krasny [9] utilize the streamfunction which can be expressed by the Laden’s transformation [1, 11]

$$\psi = \frac{\Gamma}{2\pi}(\rho_1 + \rho_2)[K(\lambda) - E(\lambda)] \quad (5)$$

where $K(\lambda)$ and $E(\lambda)$ represent complete elliptic integrals of the first and second kind, $\lambda = (\rho_2 - \rho_1)/(\rho_2 + \rho_1)$, $\rho_1^2 = (z - z_i)^2 + (r - r_i)^2$, and $\rho_2^2 = (z - z_i)^2 + (r + r_i)^2$. Here, the strength of the vortex is Γ . While the axial and radial velocities induced by a filament vortex ring can be obtained using Equation (4), the partial derivatives of ψ are given as follows:

$$\frac{\partial \psi}{\partial z} = \frac{z - z_i}{\rho_1} \frac{\partial \psi}{\partial \rho_1} + \frac{z + z_i}{\rho_2} \frac{\partial \psi}{\partial \rho_2}, \quad \frac{\partial \psi}{\partial r} = \frac{r - r_i}{\rho_1} \frac{\partial \psi}{\partial \rho_1} + \frac{r + r_i}{\rho_2} \frac{\partial \psi}{\partial \rho_2} \quad (6)$$

where

$$\frac{\partial \psi}{\partial \rho_1} = \frac{\Gamma}{2\pi} \left[K(\lambda) - \frac{1}{2} \left(1 + \frac{\rho_2}{\rho_1} \right) E(\lambda) \right], \quad \frac{\partial \psi}{\partial \rho_2} = \frac{\Gamma}{2\pi} \left[K(\lambda) - \frac{1}{2} \left(1 + \frac{\rho_1}{\rho_2} \right) E(\lambda) \right] \quad (7)$$

The solution of Nische and Krasny [9] is used as benchmark to verify the new solutions we developed using different approaches.

Another form of the streamfunction is available in References [1, 6]. We used the different ψ expression to find another form of the solution

$$\psi = \frac{\Gamma}{2\pi} \sqrt{r_i r} \left[\left(\frac{2}{\sqrt{m}} - \sqrt{m} \right) K(m) - \frac{2}{\sqrt{m}} E(m) \right] \quad (8)$$

where $m = 4rr_i/a^2$ and $a^2 = (r + r_i)^2 + (z - z_i)^2$. In this new approach, the partial derivatives of ψ are given as follows:

$$\frac{\partial \psi}{\partial z} = \left(\frac{\Gamma}{4\pi} \frac{z - z_i}{a} \right) \left[c_1 K(m) + c_2 \frac{dK(m)}{dm} + c_3 \frac{d^2 K(m)}{dm^2} \right] \quad (9)$$

$$\frac{\partial \psi}{\partial r} = \left(\frac{\Gamma}{4\pi} \frac{r + r_i}{a} \right) \left[d_1 K(m) + d_2 \frac{dK(m)}{dm} + d_3 \frac{d^2 K(m)}{dm^2} \right] \quad (10)$$

with the following coefficients $c_1 - c_3$ and $d_1 - d_3$:

$$c_1 = m + 4p, \quad c_2 = 4m(m - 1) + 4(9m - 4)p, \quad c_3 = 16m(m - 1)p \quad (11)$$

$$d_1 = m + \rho, \quad d_2 = 4m(m - 1) + (9m - 4)\rho, \quad d_3 = 4m(m - 1)\rho \quad (12)$$

where

$$p = -\frac{2rr_i}{a^2}, \quad \rho = \frac{4r_i}{(r + r_i)} + 4p \quad (13)$$

While the first derivative of $K(m)$ is identified in terms of $K(m)$ and $E(m)$,

$$\frac{dK(m)}{dm} = -\frac{K(m)}{2m} + \frac{E(m)}{2m(1 - m)} \quad (14)$$

its second derivative, $d^2 K(m)/dm^2$, must be obtained from the hypergeometric differential equation [10]

$$m(1 - m) \frac{d^2 K(m)}{dm^2} + [1 - 2m] \frac{dK(m)}{dm} - \frac{1}{4} K(m) = 0 \quad (15)$$

3. ANALYTIC SOLUTION USING BIOT-SAVART LAW

It is known that the streamfunction ψ can be written in integral form [7]

$$\psi = \frac{\Gamma}{4\pi} (rr_i) \int_0^{2\pi} \frac{\cos(\theta - \theta_i)}{|\mathbf{r} - \mathbf{r}_i|} d(\theta - \theta_i) \quad (16)$$

where

$$\begin{aligned} |\mathbf{r} - \mathbf{r}_i| &= [(z - z_i)^2 + r^2 r_i^2 - 2rr_i \cos(\theta - \theta_i)]^{1/2} \\ &= [A + B \sin \theta_i]^{1/2} \end{aligned} \quad (17)$$

where $A = (z - z_i)^2 + r^2 + r_i^2$ and $B = -2rr_i$ for an axisymmetric case (note $\theta = \pi/2$). If we substitute the integral form of ψ of Equation (16) into the curl of a vector Ψ of

Equation (2), then the Biot–Savart law [3–5] can be obtained:

$$\begin{aligned}
 \mathbf{u} &= \nabla \times \left(\frac{1}{r} \psi \hat{\mathbf{e}}_{\theta_i} \right) \\
 &= \nabla \times \left(\frac{\Gamma}{4\pi} r_i \int_0^{2\pi} \frac{-\sin \theta_i}{|\mathbf{r} - \mathbf{r}_i|} d\theta_i \hat{\mathbf{e}}_{\theta_i} \right) \\
 &= \frac{\Gamma}{4\pi} r_i \int_0^{2\pi} \frac{r_i - r \sin \theta_i}{|\mathbf{r} - \mathbf{r}_i|^3} d\theta_i \hat{\mathbf{e}}_z + \frac{\Gamma}{4\pi} r_i \int_0^{2\pi} \frac{(z - z_i) \sin \theta_i}{|\mathbf{r} - \mathbf{r}_i|^3} d\theta_i \hat{\mathbf{e}}_r
 \end{aligned} \tag{18}$$

Arranging Equation (17) to be such that $\sin \theta_i = (|\mathbf{r} - \mathbf{r}_i|^2 - A)/B$ and substituting this expression for $\sin \theta_i$ into Equation (18) yields

$$u_z = \frac{\Gamma}{4\pi} r_i \left[\left(r_i + r \frac{A}{B} \right) I_2 - \frac{r}{B} I_1 \right] \tag{19}$$

$$u_r = \frac{\Gamma}{4\pi} r_i \left(\frac{z - z_i}{B} \right) [I_1 - A I_2] \tag{20}$$

where

$$I_1 = \frac{4}{a} K(m), \quad I_2 = \frac{4}{a^3} \frac{E(m)}{(1-m)} \tag{21}$$

which completes the general formulation for the induced velocities. Equations (19) and (20) are relatively simpler than the previous solutions obtained using streamfunction approach.

4. VERIFICATION OF THE ANALYTICAL RESULTS

A numerical routine was written to compare these expressions (Equations (19) and (20)) with those obtained from differentiation of the streamfunction. The comparison was made on a ring vortex of unit strength centred at $r_i, z_i = 0.5, 0.5$. Streamline patterns and velocity vectors for this flow are shown in Figure 2. In this calculation, the elliptic integrals $K(m)$ and $E(m)$ were computed from polynomial approximations from Abramowitz and Stegun [10] which are accurate to within 2×10^{-8} . Previously, it is shown that there are three different analytical methods: (i) the streamfunction solution of Nitsche and Krasny [9], (ii) the streamfunction solution of Equations (9) and (10), and (iii) the solution by Equations (19) and (20) of the Biot–Savart law.

The streamfunction-based approach of Nitsche and Krasny [9] has been used to compare the results of the numerical solutions and the new analytical solutions. Streamline patterns for conditions used in Figure 2 are shown in Figure 3 for various Gaussian quadrature points and

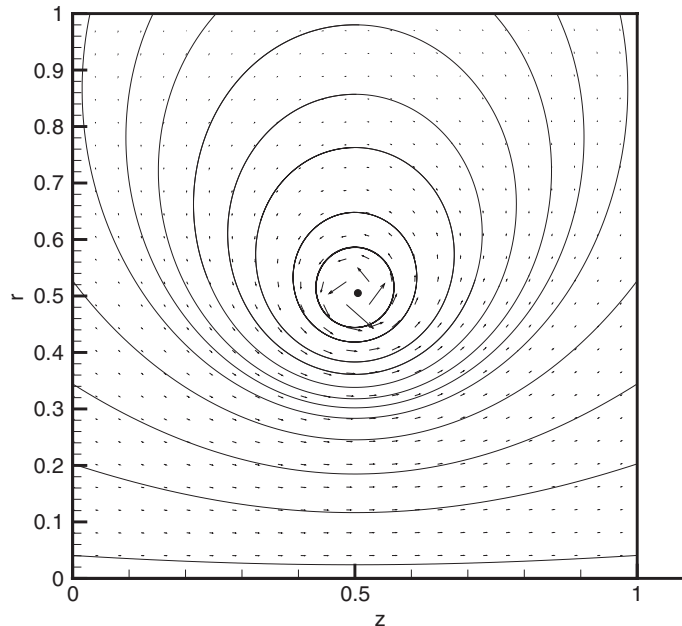


Figure 2. Streamlines and vortex-induced velocity vectors: vortex-ring location at $z_i = r_i = 0.5$.

the analytical methods. While the Gaussian integration, I , is defined as follows:

$$I = \sum_{i=1}^n w_i f(x_i) \quad (22)$$

where w_i are weighting factors and $f(x_i)$ is the integrand, we have varied the numerical resolution ($4 \leq n \leq 96$) to investigate its effect. It is shown that the results obtained by the low numerical resolution (i.e. 4 points) are not acceptable for the case used in Figure 2; it is probably due to large vortex strength. The streamline patterns with 20 Gaussian points or higher yield the result equivalent to the analytic solution of Nitsche and Krasny [9]. Results of the new analytical solution is in exact agreement with those of Nitsche and Krasny [9]. In Table I, the sample calculations with the condition used in Figure 2 are performed for an arbitrary field point, $z = r = 1.00$. The results show at least 20 Gaussian points are required to obtain the solutions within 1% accuracy. Accuracy of the new analytical solutions are within $\sim 10^{-16}$ accuracy.

Table II shows the comparison of the computational efficiency. The calculations have been performed on 2.4 GHz HP machine with LINUX environment. Field points are constructed to be such that the square grid cell does not overlap with the location of the vortex-ring $z_i = r_i = 0.5$. The grid cells (or field points) of 400×400 are used with a ring vortex of unit strength to test the efficiency comparison. The CPU time for the analytical solution is less than that of 8 Gaussian point method though the 4 Gaussian point method is faster than the analytic solution by the slightest margin. However, the 4 point method is of little practical value as it yields inaccurate results. It is shown that the analytical solutions of the Biot–Savart law is the most efficient analytical method.

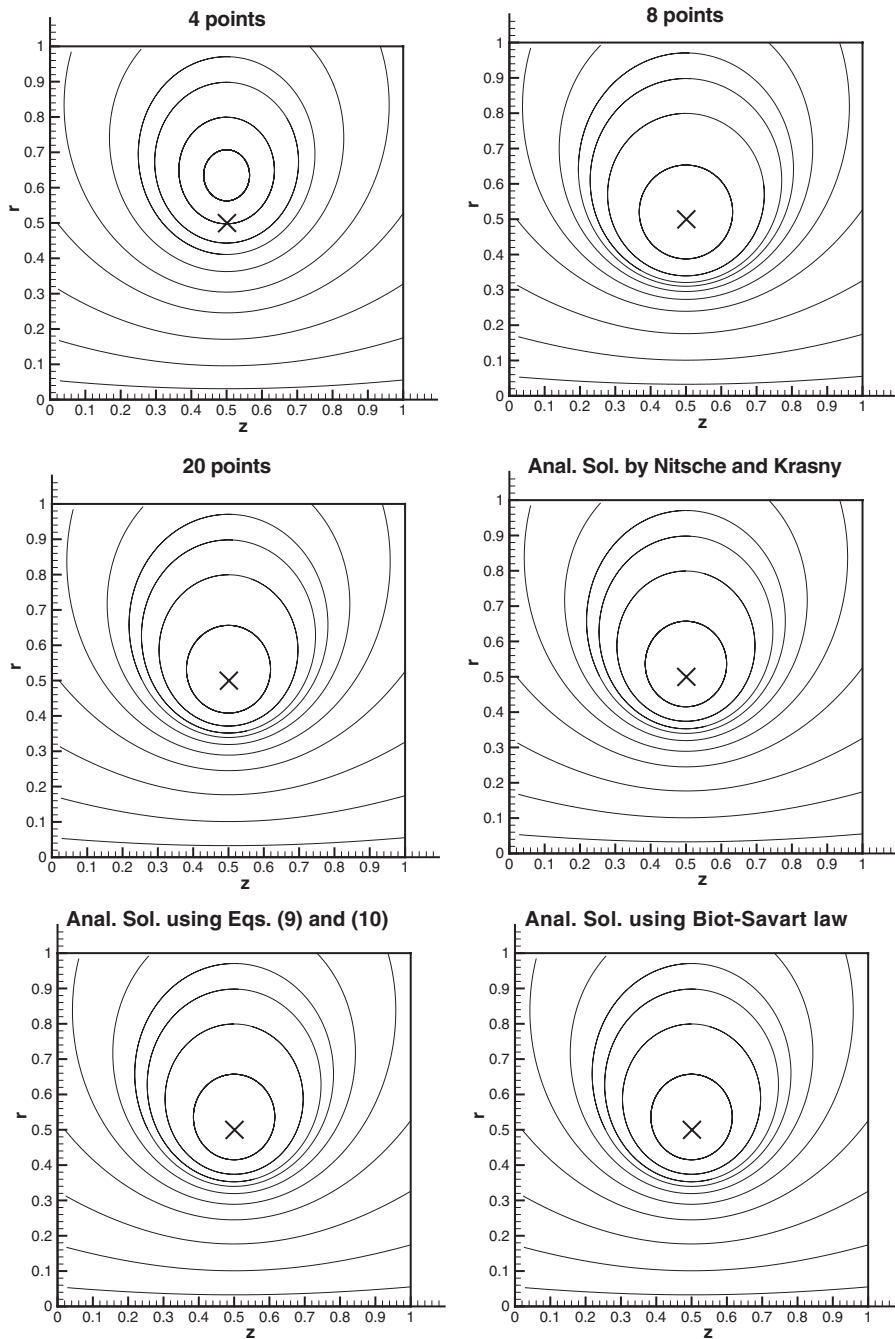


Figure 3. Streamlines comparison between Gaussian quadrature (4, 8, and 20 points) and analytic solutions. X indicates the vortex-ring location at $z_i = r_i = 0.5$.

Table I. Both numerical solutions (Gauss quad.) and the new analytical solutions are compared with the analytical solution by Nitsche and Krasny [9].

Solution methods	Error in u_z (%)	Error in u_r (%)
Gauss 4 pts. quad.	35.24	4.96
Gauss 8 pts. quad.	97.87	2.32
Gauss 20 pts. quad.	$\sim 10^{-2}$	$\sim 10^{-6}$
Gauss 40 pts. quad.	$\sim 10^{-5}$	$\sim 10^{-7}$
Gauss 64 pts. quad.	$\sim 10^{-6}$	$\sim 10^{-8}$
Gauss 96 pts. quad.	$\sim 10^{-7}$	$\sim 10^{-9}$
Anal. Sol. using Eqs. (9) and (10)	$\sim 10^{-16}$	$\sim 10^{-16}$
Anal. Sol. using Biot–Savart law	$\sim 10^{-16}$	$\sim 10^{-16}$

Table II. Comparison of the computational cost in CPU time (s).

Solution methods	CPU time (s)
Gauss 4 pts. quad.	4.535
Gauss 8 pts. quad.	5.701
Gauss 20 pts. quad.	8.416
Gauss 40 pts. quad.	13.173
Gauss 64 pts. quad.	18.796
Gauss 96 pts. quad.	19.681
Anal. Sol. by Nitsche and Krasny [9]	10.632
Anal. Sol. using Equations (9) and (10)	11.205
Anal. Sol. using Biot–Savart law	5.604

5. CONCLUSIONS

New analytic solutions for the velocity field induced by a potential vortex ring are obtained using both the streamfunction approach and the Biot–Savart law. The equivalence of the streamfunction approach and the Biot–Savart law is analytically shown. The solution from Biot–Savart law is relatively simple and computationally efficient compared to the numerical integration and other analytical methods.

REFERENCES

1. Lamb H. *Hydrodynamics*. Dover: New York, 1879; 236–239.
2. Ramsey AS. *A Treatise on Hydromechanics*. G. Bell and Sons: London, 1920; 241–244.
3. Duncan WJ, Thom AS, Young AD. *An Elementary Treatise on the Mechanics of Fluids*. Edward Arnold: London, 1960; 93–94.
4. Robertson J. *Hydrodynamics in Theory and Application*. Prentice-Hall: Englewood Cliffs, New Jersey, 1965, 128–132.
5. Karamcheti K. *Principles of Ideal-Fluid Aerodynamics*. John Wiley: New York, 1966; 526–530, 599.
6. Batchelor GK. *An Introduction to Fluid Dynamics*. Cambridge University Press: New York, 1967; 521–526.
7. Saffman PG. *Vortex Dynamics*. Cambridge University Press: New York, 1992; 192–195.
8. Panton RL. *Incompressible Flow*. Wiley: New York, 1996, 461–466.
9. Nitsche M, Krasny R. A numerical study of vortex ring formation at the edge of a circular tube. *Journal of Fluid Mechanics* 1994; **276**:139–161.
10. Abramowitz M, Stegun FA. *Handbook of Mathematical Functions*. Dover Publications: New York, 1972, 562–566, 590–592.
11. Cayley A. *An Elementary Treatise on Elliptic Functions, with Applications*. 2nd edn. Bell: London, 1895.